

Coordination Chemistry of Microbial Iron Transport Compounds. 19. Stability Constants and Electrochemical Behavior of Ferric Enterobactin and Model Complexes¹

Wesley R. Harris, Carl J. Carrano, Stephen R. Cooper, Stephen R. Sofen, Alex E. Avdeef, James V. McArdle, and Kenneth N. Raymond*

Contribution from the Department of Chemistry, University of California, Berkeley, California 94720. Received April 16, 1979

Abstract: Enterobactin, a microbial iron-transport compound with three catechol (*o*-dihydroxybenzene) groups, has been isolated from cultures of *Klebsiella pneumoniae* (formerly *Aerobacter aerogenes*) and studied by potentiometric, spectrophotometric, and electrochemical techniques. The enterobactin model compound *N,N*-dimethyl-2,3-dihydroxybenzamide (DMB) has also been examined, and the results of that examination have been employed in analysis of the enterobactin data. The stepwise equilibrium constants ($\log K$) for successive addition of DMB dianion to a ferric ion are 17.77 (4), 13.96 (2), and 8.51 (3), respectively, for an overall formation constant of 40.2 (1). The proton-dependent stability constant K^* for ferric enterobactin (H_6ent) has been determined spectrophotometrically by competition vs. EDTA to be $10^{-9.7(3)}$, where $K^* = ([Fe(ent)^{3-}][H^+]^6)/([Fe^{3+}][H_6ent])$. We have approximated the protonation constants of enterobactin based on those of the model compound DMB, and thereby estimated a value for the conventional (proton-independent) formation constant ($\log K_f$) of 52, where $K_f = [Fe(ent)^{3-}]/([Fe^{3+}][ent^{6-}])$. This is the largest formation constant reported for a ferric complex. The $[Fe(ent)]^{6-}$ complex undergoes a series of 1:1 protonations to yield sequentially $[Fe(Hent)]^{2-}$, $[Fe(H_2ent)]^-$, and $[Fe(H_3ent)]$. The chelate protonation constant for the first of these steps has been calculated to be $\log K_{MHL} = 4.89$ (6), where $K_{MHL} = [Fe(Hent)]/([Fe(ent)][H^+])$. These protonation reactions correspond to a conversion from a catecholate to salicylate mode of bonding at low pH. Electrochemical study of the ferric enterobactin complex by cyclic voltammetry demonstrates that it is reversibly reduced at pH values above 10, with a formal potential of -986 mV vs. normal hydrogen electrode (NHE) (at pH 10). At lower pH values the reduction potential increases with decreasing pH, leading to an estimated value of -750 mV at pH 7. The physiological implications of these results are discussed.

Introduction

Iron acquisition presents profound difficulties for aerobic microorganism due to the insolubility of ferric hydroxide, the equilibrium concentration of which is 10^{-18} M at pH 7.² As a response to this environmental stress, bacteria evolved siderophores, low-molecular-weight chelates that solubilize ferric ion for transport into the cell. The siderophores generally can be divided into two classes: those based on hydroxamate chelating groups and those based on catechol groups.³ The first hydroxamate-based siderophore was discovered in 1952 by Neilands⁴ and subsequently received considerable attention, prompted in part by interest in these ligands for possible clinical application in treatment of iron poisoning and for use as antibiotics.⁵ In 1970, enterobactin (Figure 1), a catechol-based siderophore, was isolated from *Escherichia coli* by O'Brien and Gibson⁶ (who named the compound enterochelin) and from *Salmonella typhimurium* by Pollack and Neilands⁷ (who named the compound enterobactin). Enterobactin, which can be isolated from several enteric bacteria, consists of a cyclic triester of 2,3-dihydroxybenzoylserine.

Each enterobactin molecule transports one ferric ion into a bacterium, where the ester linkages are enzymatically hydrolyzed;^{8,9} this hydrolysis is necessarily irreversible since the bacteria are unable to use the hydrolysis product to resynthesize enterobactin.^{9,10} Enterobactin destruction contrasts with the hydroxamate siderophores, which can shuttle many ferric ions into the cell, and from which Fe(III) release is thought to occur by simple reduction to the weakly bound ferrous complex.¹¹ These observations led to the suggestion that the reduction potential of intact ferric enterobactin is too low to allow the complex to be physiologically reduced.⁹ Thus, the electrochemical behavior of the siderophores bears directly on the postulated physiological release mechanism, and to this end we report here the results of electrochemical studies of ferric enterobactin.

Enterobactin presents exceptional difficulties for quantitative equilibrium studies. The free ligand is prone to air ox-

idation of the catechol groups, and the ester linkages are extremely susceptible to base-catalyzed hydrolysis, negating attempts to measure directly ligand acid association constants. Enterobactin complexes with metal ions are less sensitive to hydrolysis, but still present formidable obstacles to detailed study. Even the Fe(III) enterobactin stability constant, a fundamental datum for a siderophore, was not previously known, in contrast to the extensively studied hydroxamate siderophores.

The Fe(III) enterobactin stability constant takes on new importance in light of the suggestion that the success of a bacterial infection may depend critically on the ability of the microorganism to compete with its host for iron; the concept of nutritional immunity developed by Kochan entails this competition for essential nutrients.¹² Hence, the avidity with which enterobactin binds iron possesses clinical ramifications.

We have previously published preliminary reports that compared ferric enterobactin with ferric hydroxamate electrochemistry (and discussed the implications for the intracellular iron release mechanism)¹³ and which reported the spectrophotometric evaluation of the ferric enterobactin stability constant.¹⁴ To assess further the physiological role of enterobactin (specifically, its affinity for ferric ion and the mechanism of iron release), we now report the complete results of an electrochemical, potentiometric, and spectrophotometric study of ferric enterobactin and a closely related model system, *N,N*-dimethyl-2,3-dihydroxybenzamide (DMB).

Experimental Section

Preparation of Compounds. Enterobactin was extracted from 5-L batches of culture media of *Klebsiella pneumoniae* (formerly *Aerobacter aerogenes*) according to the method of Pollack and Neilands.⁷ Yields between 20 and 30 mg of enterobactin per L of culture media were obtained. Enterobactin was purified by dissolving the crude material in ethyl acetate and extracting several times with 0.1 M phosphate buffer from which iron had been removed by passage through a Chelex-100 column (Bio-Rad). The ethyl acetate solution

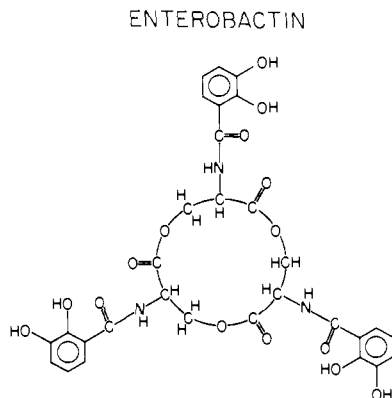


Figure 1. Structural formula of enterobactin.

was reduced in volume and the enterobactin precipitated by addition of hexane. The resulting white powder gave a single spot upon thin-layer chromatography (silica gel plates eluted with $\text{CHCl}_3/\text{MeOH}$, 5:1) and was stored in a vacuum desiccator to avoid slow air oxidation.

Solutions of $[\text{Fe}(\text{ent})]^{3-}$ were prepared immediately before use by the following procedure: equimolar amounts of FeCl_3 and enterobactin were dissolved in 95% ethanol, following which 6 equiv of 1 M aqueous KOH was added. The reaction mixture was stirred for a few minutes and passed through a Millipore filter, and the filtrate was evaporated under vacuum at 40 °C. After dissolution in water and elution from a 20×1 cm Bio-Rex 70 column, the fractions containing the complex were evaporated, taken up in 20% MeOH/ H_2O , and passed down a neutral alumina column. The $[\text{Fe}(\text{ent})]^{3-}$ in 20% MeOH/ H_2O obtained was evaporated under reduced pressure at room temperature to remove the methanol, and the final $[\text{Fe}(\text{ent})]^{3-}$ concentration determined spectrophotometrically from the absorbance at 495 nm (ϵ 5600).¹⁵

The complex was characterized by UV-vis absorption spectroscopy (Cary 118 spectrophotometer) and by thin-layer chromatography (Kieselgel D-O silica gel on coated glass plates). The potassium salt of ferric enterobactin in methanol solution was chromatographed using 6:5 chloroform/methanol and stained with iodine vapor. A solution of $[\text{Fe}(\text{ent})]^{3-}$ yielding a single spot with an R_f of 0.75 was accepted as a pure preparation.

Ligand Hydrolysis. Hydrolysis studies on free enterobactin were based on the procedure of Greenwood and Luke.¹⁶ Over a 12-h period, aliquots of an aqueous solution of enterobactin at pH 5 were removed and extracted with ethyl acetate; both layers were diluted to standard volume and analyzed spectrophotometrically at 315 nm. The hydrolysis products are anionic at pH 5 and thus water soluble, while the unhydrolyzed enterobactin is extracted into the organic layer, so that hydrolysis results in a loss of intensity in the ethyl acetate fraction and a corresponding increase in the aqueous layer. At the end of the run, the pH was raised to 12, then brought back to 5 as quickly as possible. The ethyl acetate fraction then showed essentially no absorbance at 315 nm, indicating complete hydrolysis of the enterobactin.

Potentiometric Titrations. The apparatus and procedures for potentiometric measurements have been previously described in detail.¹⁷ Briefly, measurements were made at 25 °C and 0.10 M ionic strength (KNO_3) with a pH meter standardized (with nitric and acetic acid) to read hydrogen ion concentration instead of activity.

Ferric enterobactin solutions for potentiometric titration were quantitated spectrophotometrically, diluted to 40 mL, and titrated with standardized nitric acid under an argon atmosphere after addition of the appropriate amount of KNO_3 and a small amount of KOH (to ensure the titration would not begin on a sharp inflection).

Refinement of the potentiometric data was performed by a non-linear least-squares program, which varied the set of equilibrium constants to minimize the function:

$$R = \sum w^2(\text{pH}_{\text{obsd}} - \text{pH}_{\text{calcd}})^2 \quad (1)$$

The weighting factor w^2 is defined by:

$$\left(\frac{1}{w}\right)^2 = [\sigma(\text{pH})]^2 = \sigma_c^2 + \sigma_v^2 \left(\frac{\partial \text{pH}}{\partial V}\right)^2 \quad (2)$$

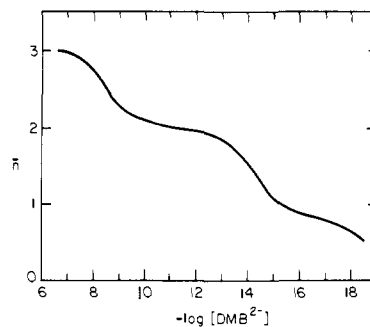


Figure 2. Bjerrum plot for iron(III) in the presence of an 11-fold excess of 2,3-dihydroxy-*N,N*-dimethylbenzamide (DMB), where \bar{n} represents the average number of ligands bound to the metal.

where the standard deviation of any given pH measurement, $\sigma(\text{pH})$, is determined by the intrinsic error in pH measurement, σ_c , plus the error resulting from an error in the volume of titrant delivered (0.002 mL), which is propagated by the slope of the titration curve at pH_{obsd} , $\partial \text{pH} / \partial V$. This weighting scheme minimizes the importance of the less reliable data from regions of steep slope relative to the data from the buffer regions.

Spectrophotometric Titrations. Samples for spectrophotometric measurements were prepared as described above, except that the intense visible absorbance of $[\text{Fe}(\text{ent})]^{3-}$ necessitated more dilute solutions. In the spectrophotometric titrations the pH was adjusted in small increments by the addition of nitric acid, and after the pH stabilized (less than 5 min), an aliquot was removed and its visible spectrum recorded.

Spectrophotometric competition experiments were performed with 10-mL samples that were 0.1 mM each in enterobactin and ferric ion with up to an eightfold excess of EDTA (which served to buffer the solutions at about pH 5). Equilibrium was approached from both directions; i.e., free EDTA was added to a ferric enterobactin solution or, alternatively, free enterobactin was added to a solution of ferric EDTA. Owing to its low water solubility, the free enterobactin was added as 0.3–0.5 mL of a concentrated methanol solution. The visible spectra of these solutions were then recorded at periodic intervals until there was no further change with time, which required 8–10 h.

Electrochemistry. The electrochemical methods used have been described previously.¹³

Infrared Spectra. Solid-state spectra were run as KBr pellets on a Perkin-Elmer Model 576 spectrometer. Solution spectra of ~ 0.05 M D_2O solutions were collected (200 scans) on a Nicolet 7000 FT-IR spectrometer using 0.05-mm path length AgCl plates. The pD of the samples was adjusted with NaOD (prepared from metallic sodium and D_2O) or DCl (prepared from hydrolysis of PCl_3 with D_2O).

Results

DMB. Potentiometric Titrations. The facility with which enterobactin hydrolyzes at high pH prevents direct determination of the ligand protonation constants and necessitates their estimation based on the values for the bidentate analogue DMB (*N,N*-dimethyl-2,3-dihydroxybenzamide). Determination of the DMB protonation constants by potentiometric titration yields values of $\log K_1^{\text{H}} = 12.1$ and $\log K_2^{\text{H}} = 8.42$ (1), where the constants are expressed as:

$$K_n^{\text{H}} = \frac{[\text{H}_n\text{L}]}{[\text{H}_{n-1}\text{L}][\text{H}^+]} \quad (3)$$

Since it is difficult to obtain accurate values of very high protonation constants from potentiometric data, the error in $\log K_1^{\text{H}}$ is probably around ± 0.3 .

To prevent precipitation of ferric hydroxide, the Fe^{III} DMB solutions contained a sixfold excess of DMB, and thus the resulting titration curve reflects both complexation and ligand deprotonation equilibria. However, the Bjerrum plot for the ferric DMB system, shown in Figure 2, clearly indicates the stepwise formation of the ferric mono-, bis-, and tris(DMB) complexes. Refinement of these potentiometric data yielded

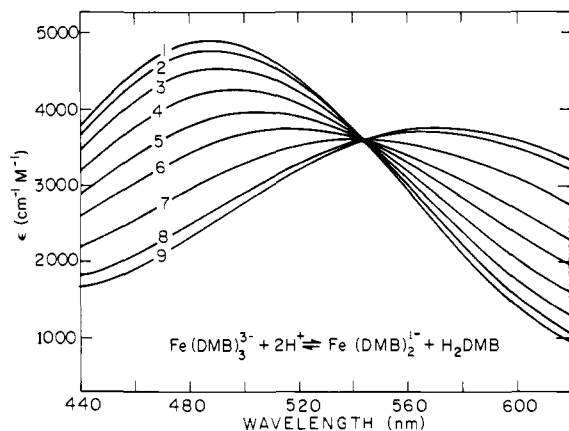


Figure 3. Visible spectra of a 10:1 DMB-Fe³⁺ solution as a function of pH: (1) pH 8.94; (2) 7.94; (3) 7.58; (4) 7.37; (5) 7.21; (6) 7.07; (7) 6.85; (8) 6.52; (9) 6.07.

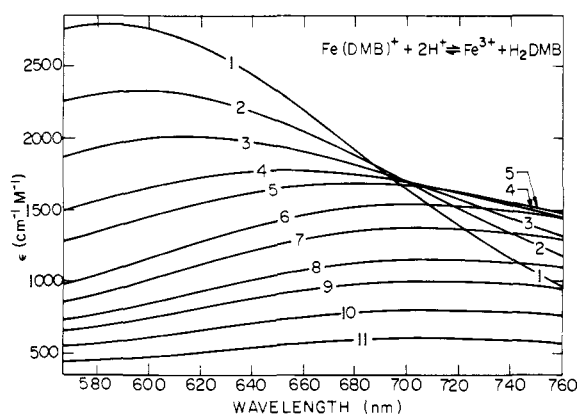
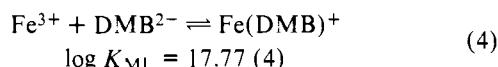
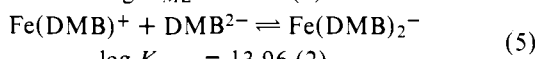


Figure 4. Visible spectra of a 10:1 DMB-Fe³⁺ solution as a function of pH: (1) pH 4.68; (2) 4.47; (3) 4.33; (4) 4.14; (5) 3.99; (6) 3.64; (7) 3.40; (8) 3.06; (9) 2.83; (10) 2.60; (11) 2.41.

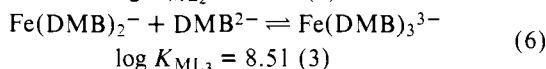
the results shown below (eq 4-7).



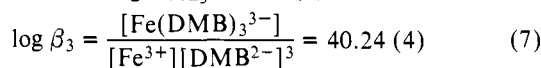
$$\log K_{\text{ML}} = 17.77 \quad (4)$$



$$\log K_{\text{ML}_2} = 13.96 \quad (2)$$



$$\log K_{\text{ML}_3} = 8.51 \quad (3)$$



Spectrophotometric Titration Results. The pH dependence of the ferric DMB visible spectrum also reflects the presence of three sequential complexation reactions. The [Fe(DMB)₃]³⁻ complex gives a deep red solution with λ_{max} 488 nm (ϵ 4910). As the pH is lowered from 8.6 to 6.0, the spectra exhibit a sharp isosbestic point at 543 nm, as shown in Figure 3, which results from the overlap of the absorption bands of [Fe(DMB)₃]³⁻ and [Fe(DMB)₂]⁻ (as per eq 6). Owing to the wide separation between the buffer regions, the spectrum at pH 6 is essentially that of the bis(DMB) complex, which has a band maximum at 570 nm with an ϵ of 3750. As the pH is lowered further from 6 to 4.8, a new isosbestic point forms at 688 nm, now reflecting the overlap of the spectra of [Fe(DMB)₂]⁻ and [Fe(DMB)]⁺ (eq 5). The further decrease in pH shifts λ_{max} to 710 nm and results in a continuous decrease in intensity, as shown in Figure 4, which indicates the complete dissociation of the [Fe(DMB)]⁺ complex to hexaquoiron(III) and free DMB (eq 4).

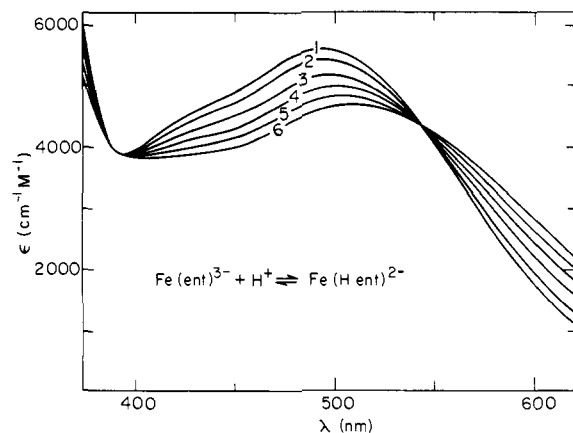


Figure 5. Visible spectra of ferric enterobactin as a function of pH: (1) pH 7.29; (2) 5.66; (3) 5.11; (4) 4.80; (5) 4.53; (6) 4.23.

Because of the overlap between the two equilibria defined by eq 4 and 5, it is not possible simply to measure the spectrum of the 1:1 [Fe(DMB)]⁺ species. However, the extinction coefficient of this complex is known at the 688-nm isosbestic point. Therefore, the value of K_{ML} can be determined from the low pH spectra by use of $\epsilon_{\text{ML}}^{688} = 1940$ to calculate [Fe(DMB)]⁺ and by the combination of this result with the appropriate mass balance equations to obtain [Fe³⁺] and [DMB²⁻]. Hydrolysis of free ferric ion has been included, so that [Fe³⁺] denotes the concentration of unhydrolyzed hexaquoiron(III). The spectral data give a value of $\log K_{\text{ML}} = 17.95$, compared to 17.77 from the titration data.

Given the value of $\log K_{\text{ML}}$, it is possible to calculate the extinction coefficient for [Fe(DMB)]⁺ at 568 nm, and the λ_{max} of the [Fe(DMB)₂]⁻ complex. Then the ferric DMB system between pH 4 and 6 can be described by the set of equations:

$$\text{abs}^{568} = \epsilon_{\text{ML}_2} [\text{ML}_2] + \epsilon_{\text{ML}} [\text{ML}] \quad (8)$$

$$[\text{Fe}]_{\text{tot}} = [\text{ML}_2] + [\text{ML}] \quad (9)$$

$$[\text{DMB}]_{\text{tot}} = 2[\text{ML}_2] + [\text{ML}] + \alpha_{\text{L}}[\text{L}] \quad (10)$$

which have been used to calculate a value of $\log K_{\text{ML}_2}$ of 13.97 (4), in good agreement with the potentiometric value of 13.96. The solution of equations analogous to 8-10, which describe the Fe(DMB)₂-Fe(DMB)₃ system, gives $\log K_{\text{ML}_3} = 8.90$ (7), also in reasonable agreement with the potentiometric value of 8.51.

Enterobactin. Spectrophotometric Titration Results. The visible spectrum of ferric enterobactin does not change above pH 7, which indicates that the red, hexacoordinate [Fe(ent)]³⁻ complex is fully formed at this pH, in agreement with the titration results (vide infra). As the pH is lowered from 7 to 4.2, a sharp isosbestic point appears at 542 nm (Figure 5), consistent with a simple equilibrium between two metal complexes absorbing in the visible region. However, unlike the DMB system, these spectra do not represent the dissociation of a ligand, but rather the single-step protonation of the ferric enterobactin complex. The equations shown below describe such a process for the addition of an unknown number of protons to ferric enterobactin:

$$\text{abs} = \epsilon_{\text{ML}} [\text{ML}] + \epsilon_{\text{MH}_n\text{L}} [\text{MH}_n\text{L}] \quad (11)$$

$$[\text{Fe}]_{\text{tot}} = [\text{ML}] + [\text{MH}_n\text{L}] \quad (12)$$

$$K_{\text{MH}_n\text{L}} = \frac{[\text{MH}_n\text{L}]}{[\text{ML}][\text{H}^+]^n} \quad (13)$$

The sole assumption made here is that there are only two species present, Fe(ent) and Fe(H_nent), as indicated by the

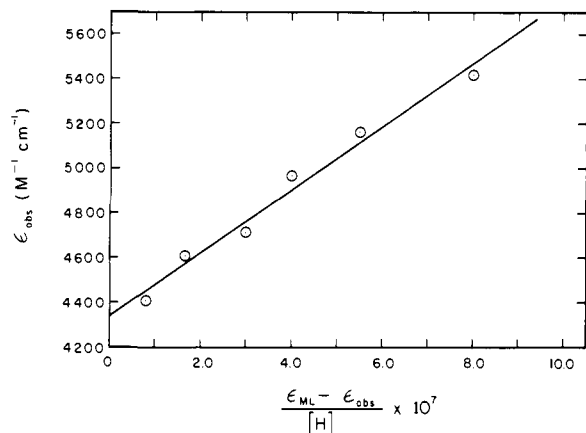


Figure 6. Plot of ϵ_{obsd} vs. $(\epsilon_{\text{ML}} - \epsilon_{\text{obsd}})/[\text{H}]$ for ferric enterobactin at 495 nm, where ϵ_{obsd} is the absorbance at any pH divided by the analytical iron concentration, and ϵ_{ML} is the molar extinction coefficient of the $[\text{Fe}(\text{ent})]^{3-}$ complex. Such a plot using $1/[\text{H}]$ to the first power is for the addition of a single proton to the ferric enterobactin complex, and the slope is then equal to $1/K_{\text{MHL}}$.

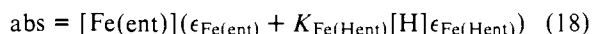
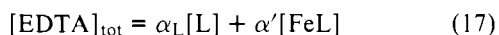
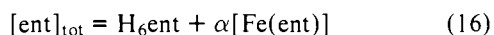
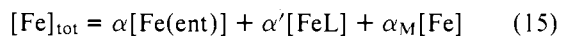
isosbestic point. Rearrangement of eq 11–13 gives:

$$\epsilon_{\text{obsd}} = \epsilon_{\text{MH}_n\text{L}} + \frac{(\epsilon_{\text{ML}} - \epsilon_{\text{obsd}})}{K_{\text{MH}_n\text{L}}[\text{H}]^n} \quad (14)$$

where $\epsilon_{\text{obsd}} = \text{abs}/[\text{Fe}]_{\text{tot}}$. Graphs of ϵ_{obsd} vs. $(\epsilon_{\text{ML}} - \epsilon_{\text{obsd}})/[\text{H}]^n$ are linear only for $n = 1$ (Figure 6), which indicates that ferric enterobactin reacts with a single hydrogen ion to form an $[\text{Fe}(\text{Hent})]^{2-}$ complex; the slope of the line yields $\log K_{\text{MHL}} = 4.89$ (6).

Protonation of ferric enterobactin in discrete one-proton steps provides a reasonable explanation for the precipitation of an iron complex at pH 3, since addition of three protons to ferric enterobactin yields the neutral $\text{Fe}(\text{H}_3\text{ent})$ complex, which is expected to be sparingly soluble in water.

Competition Experiments. The formation constant of ferric enterobactin cannot be determined from the titration data alone because the complex is essentially fully formed over the entire pH range accessible to titration without precipitation. For this reason, the ferric enterobactin proton-dependent stability constant was determined spectrophotometrically by competition with EDTA. A mixture of ferric ion, enterobactin, and EDTA (L) between pH 4.2 and 6 is described by the equations:



Assuming that $[\text{Fe}^{3+}] \approx 0$ (due to the excess ligand present), these equations have been solved for $[\text{Fe}(\text{ent})]$, $[\text{Fe}(\text{EDTA})]$, $[\text{H}_6\text{ent}]$, and $[\text{EDTA}^{4-}]$, and these quantities were used to calculate the distribution coefficient K_x , where:

$$K_x = \frac{[\text{Fe}(\text{ent})^{3-}][\text{H}]^6[\text{EDTA}^{4-}]}{[\text{Fe}(\text{EDTA})^-][\text{H}_6\text{ent}]} = \frac{K^*}{K_{\text{FeEDTA}}} \quad (19)$$

The K_{FeEDTA} represents the normal formation constant of ferric EDTA, and thus K^* is defined as:

$$K^* = \frac{[\text{Fe}(\text{ent})^{3-}][\text{H}]^6}{[\text{Fe}^{3+}][\text{H}_6\text{ent}]} \quad (20)$$

This equilibrium has been approached from both directions, i.e., adding EDTA to ferric enterobactin as well as by adding enterobactin to ferric EDTA, to assure attainment of equilibrium. Eight solutions starting with ferric enterobactin gave

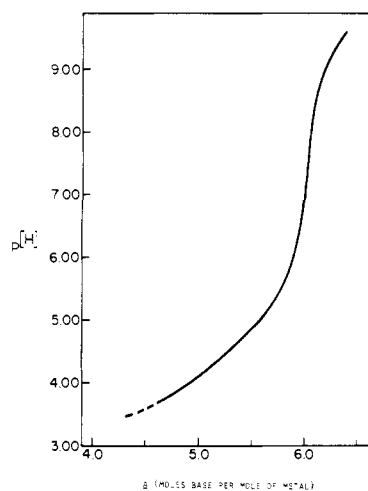


Figure 7. Potentiometric equilibrium curve of ferric enterobactin. The dashed line below pH 3.7 indicates precipitation of a protonated iron-enterobactin complex.

a value of K^* of $10^{-9.6(2)}$, while another set of eight solutions starting with ferric EDTA yielded $K^* = 10^{-9.8(4)}$. The difference between the two means lacks statistical significance at the 90% level, as shown by a standard F test.¹⁸

Because the competition solutions required 8–10 h to equilibrate, there was some concern that significant amounts of free enterobactin might be hydrolyzed during the course of the experiment. Therefore, enterobactin hydrolysis in 0.10 M KNO_3 at pH 5 and 25 °C was followed spectrophotometrically, and it was observed that less than 5% of the ligand hydrolyzed in 12 h. In the competition solutions only 20–30% of the total enterobactin is present as the free ligand, so the extent of hydrolysis in these solutions is probably well below the 5% level and should not be a factor.

Potentiometric Titration Results. The titration curve of ferric enterobactin (Figure 7) is essentially featureless, and only indicates that the six phenolic protons are displaced by $\text{Fe}(\text{III})$ above pH 7.4. Formation of an isolable purple precipitate prevents extension of the titration below pH 3.8; the purple material does not, however, constitute a degradation product, since its dissolution in pH 10 buffer regenerates the original $[\text{Fe}(\text{ent})]^{3-}$ complex. Two chelate protonation constants were calculated by least-squares refinement of the titration data from pH 3.8 to 5, with the values shown in eq 21 and 22.

$$K_{\text{MHL}} = \frac{[\text{Fe}(\text{Hent})]}{[\text{Fe}(\text{ent})][\text{H}]} = 10^{4.80(1)} \quad (21)$$

$$K_{\text{MH}_2\text{L}} = \frac{[\text{Fe}(\text{H}_2\text{ent})]}{[\text{Fe}(\text{Hent})][\text{H}]} = 10^{3.15(1)} \quad (22)$$

Infrared Spectra. The solid-state infrared spectrum of free enterobactin contains bands at 1750 (ester $\nu_{\text{C}=\text{O}}$), 1638 (amide I), 1583, 1530, and 1455 cm^{-1} (skeletal modes, $\nu_{\text{C}=\text{C}}$ of the phenyl ring). In the solid-state spectrum of the red ferric enterobactin complex, the amide I band shifts from 1638 to 1615 cm^{-1} , and the skeletal modes appear at 1580, 1535, and 1460 cm^{-1} . A new band appearing at 1440 cm^{-1} is also assigned as a $\nu_{\text{C}=\text{C}}$ skeletal mode. In D_2O solution (pD 10.1), ferric enterobactin has bands at 1595 (amide I), 1583, 1547, 1483, and 1445 cm^{-1} ($\nu_{\text{C}=\text{C}}$ skeletal modes). A previous resonance Raman study of ferric enterobactin by Spiro et al.¹⁹ showed resonance enhanced bands at 1585, 1542, and 1482 cm^{-1} , which were assigned to $\nu_{\text{C}=\text{C}}$ skeletal modes.

On lowering the pD of a D_2O solution of ferric enterobactin to 5.3, the amide I band decreases in intensity and a new band appears at 1457 cm^{-1} , with no other changes observable. At pD 4.0, the amide I band is a barely visible shoulder at 1600

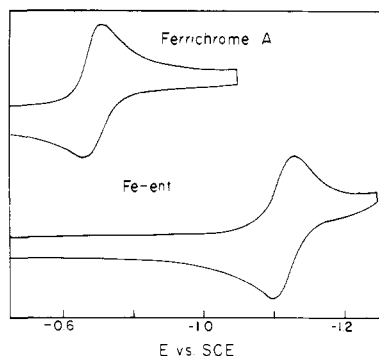


Figure 8. Cyclic voltammograms of ferrichrome A (pH 8) and ferric enterobactin (pH 10.5). All solutions are 1 M KCl with 0.05 M sodium borate–0.05 M sodium phosphate buffer.

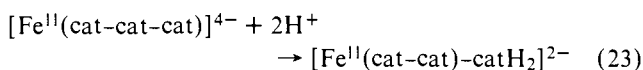
cm^{-1} , and a new shoulder appears at 1623 cm^{-1} , which corresponds to the amide I stretch in a pendant dihydroxybenzoyl (DHB) side group. Finally, with a decrease in pH to ~ 2 , the amide I band at 1600 cm^{-1} disappears completely and the band at 1624 cm^{-1} becomes clearly observable, as does the 1460-cm^{-1} band.

Electrochemistry. The cyclic voltammogram (CV) of ferric enterobactin at pH 10.5 (Figure 8) shows a reversible one-electron wave with $E_f = -1.230 \text{ V}$ vs. saturated calomel electrode (SCE). The criterion of reversibility applied was the scan-rate independent separation between the cathodic and anodic waves. Below pH 10, the cyclic voltammograms exhibit a 120 mV/pH unit increase in formal potential with decrease in pH (Table I), and become progressively more irreversible with decreasing pH. Cyclic voltammetry of ferric enterobactin solutions following hydrolysis at pH 12 shows reduction waves attributable to the ferric complex of the intact cyclic triester, and the ligand with one, two, or three ester linkages hydrolyzed, in order of increasing reduction potential. Ester hydrolysis progressively raises the reduction potential, making the ferric ion easier to reduce.

Preparative reduction of ferric enterobactin reversibly yields colorless solutions, where the ligand to metal charge transfer of the ferric complex is absent, establishing that simple reduction of the ferric ion takes place, without attack on the ligand.

Discussion

Electrochemistry. The cyclic voltammetric behavior observed for ferric enterobactin at pH 10.5 is consistent with that expected for a reversible one-electron couple.²⁰ The peak potential separation is 60 mV, whereas $59/n \text{ mV}$ is expected for a reversible n -electron couple. The remarkable feature of the ferric enterobactin CV is the very low reduction potential observed, -1.230 V vs. SCE (-0.986 V vs. normal hydrogen electrode (NHE)). The pH dependence observed is attributable to the protonation and ultimate dissociation of one of the catechol groups in the ferrous complex, according to the overall stoichiometry:



For this case, the observed formal reduction potential should vary as:

$$E_f = E_{\text{Fe}^\circ} - 59 \log \frac{K_{\text{ox}}}{K_{\text{red}}} + 59 \log (1 + K_1[\text{H}^+] + K_1K_2[\text{H}^+]^2) \quad (24)$$

where E_{Fe° is the standard reduction potential of the aquo $\text{Fe}(\text{III})/(\text{II})$ couple, K_{ox} and K_{red} are the stability constants

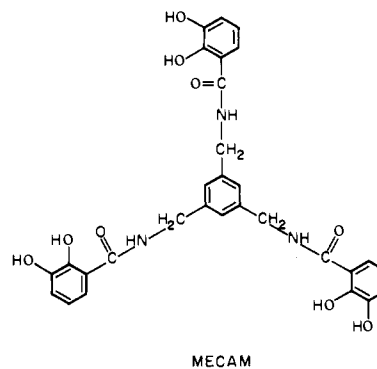


Figure 9. Structural formula of 1,3,5-*N,N',N''*-tris(2,3-dihydroxybenzoyl)triaminomethylbenzene (MECAM).

Table I. pH Dependence of $\text{Fe}(\text{III})$ Enterobactin Reduction Potentials

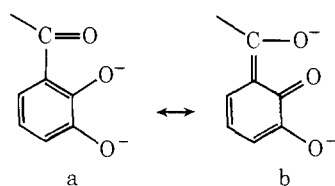
pH	E vs. SCE	ΔE
10.92	-1.230	60
10.79	-1.230	60
10.69	-1.230	60
10.56	-1.225	60
10.46	-1.222	60
10.36	-1.220	62
10.26	-1.215	65
10.13	-1.213	65
10.04	-1.210	62
9.95	-1.205	65
9.87	-1.200	65
9.73	-1.190	70
9.60	-1.178	90

of the ferric and ferrous hexacoordinate complexes, and the K_f s are the chelate protonation constants of the ferrous complex. As indicated above, only the onset of the pH-dependent region is accessible before the increasing irreversibility of the CVs prevents accurate formal potential measurements. Nevertheless, we have extrapolated the formal potential data to pH 7 and estimate the physiologically relevant pH 7 potential to be -750 mV vs. NHE. Such a value is well below the potential of reductants available *in vivo* and supports the hypothesis that enterobactin hydrolysis, with its attendant increase in reduction potential, is necessary to permit intracellular reduction and release of the ferric ion.

Enterobactin. Evidence from a variety of physicochemical techniques in our laboratory has established that in the red complex of ferric enterobactin, which is fully formed by pH 7, the iron is bound exclusively through the six phenolic oxygens of the three DHB groups. Previous results on catechol²¹ and the results presented here on DMB clearly show that the bidentate catecholate ligands form only the simple mono, bis, and tris complexes. Therefore, we initially assumed that protonation of the ferric enterobactin complex would also involve a two-proton step, generating a complex in which the iron is bound to two waters and the phenolic oxygens of two DHB groups. Our results cast doubt on this assumption and have led us to reject it in favor of salicylate-type bonding at low pH, where protonation of the meta phenolate group results in a change in the mode of bonding such that the iron coordinates through the carbonyl and deprotonated ortho phenolate oxygens.

Spectrophotometric Results. The spectrophotometric results reported here reveal that ferric enterobactin is protonated in discrete *one-proton* steps, as also occurs in the case of the tricatecholate model compound 1,3,5-*N,N',N''*-tris(2,3-dihydroxybenzoyl)triaminomethylbenzene (MECAM),²² which is shown in Figure 9. A broad charge-transfer band appears

Scheme I



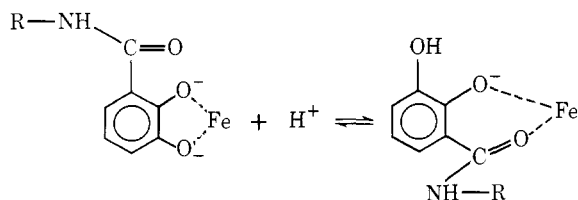
in the tris(catecholate) type complexes of enterobactin, MECAM, and DMB at 490–495 nm (ϵ 4900–5600) at pH >8. Upon addition of 2 equiv of hydrogen ion to the system, the absorption maximum of the DMB complex shifts to 570 nm, with an isosbestic point at 542 nm. In contrast, the band maxima of the ferric complexes of the macrochelate ligands enterobactin and MECAM shift only to about 510 nm upon addition of *one* proton (isosbestic point preserved), and addition of the second proton to the MECAM complex results in a further shift to only 523 nm. Thus, at no point does the characteristic spectrum of the bis(catecholate) type complex (λ_{\max} 570 nm) appear, which implies that each proton is going onto a *different* DHB group, resulting in a salicylate type bonding. Tait²³ has isolated an iron binding compound from *Paracoccus denitrificans* that contains two DHB groups conjugated to the terminal nitrogens of a spermidine molecule (1,5,10-triazadecane), with the central nitrogen attached to a 2-hydroxybenzoyl-*N*-l-threonine. This compound can bind iron only via a bis(catecholate)-mono(salicylate) type structure and has a λ_{\max} at 515 nm. This is similar to that observed for the monoprotonated ferric enterobactin complex, for which we postulate the same type of bonding.

At a pH corresponding to the addition of ~ 3 protons, an insoluble iron-containing complex precipitates from solutions of both ferric enterobactin and ferric MECAM, which in the latter case is essentially quantitative. (In both cases the precipitates redissolve in pH 10 buffer to regenerate the spectrum of the red $[\text{FeL}]^{3-}$ complex.) This insolubility at low pH suggests the formation of a neutral $[\text{FeH}_3\text{L}]$ species upon the addition of three protons to ferric enterobactin, consistent with the spectroscopic results, which indicate that the enterobactin complex is protonated in one-proton steps.

Infrared Spectra. The solution infrared spectra in D_2O as a function of pD provide additional evidence supporting the shift to a salicylate mode of bonding. Upon metal complexation at high pD, the free ligand amide I band (mainly $\nu_{\text{C}=\text{O}}$) at 1638 cm^{-1} shifts to 1615 cm^{-1} in the solid state and 1595 cm^{-1} in D_2O solution (pD 9.7). This decrease in frequency is attributable to the increased conjugation of the amide carbonyl into the aromatic system. The proton NMR results of Llinas et al.²⁴ show that upon chelation the participation of the tautomer b in Scheme I becomes significant. Since form b results in a reduction in the double bond character of the carbonyl group, a lowering of the frequency is expected.

As the pD is lowered to 5.4 (which corresponds to the addition of about 0.25 equiv of acid), the amide I band at 1600 cm^{-1} decreases in intensity, and becomes a shoulder on the 1585-cm^{-1} C–C stretch. This is consistent with a metal-carbonyl oxygen interaction, such as that postulated in Scheme II, which lowers the carbonyl stretching frequency. Typical

Scheme II



$$K_{\text{sal}} = \frac{[\text{Fe}(\text{DMB})_2(\text{HDMB})^{2-}]}{[\text{Fe}(\text{DMB})_2^{3-}][\text{HDMB}^-]} = 10^{2.5} \quad (25)$$

shifts of $20\text{--}40\text{ cm}^{-1}$ are observed upon coordination of peptide carbonyls,^{25,26} which would place the shifted band under the benzene ring skeletal modes. Addition of 2 equiv of deuterium ion (pD 4) decreases the amide I band further in intensity, so that it is only a weak shoulder, and a new band appears at 1623 cm^{-1} , indicative of an uncoordinated DHB. Finally, at pD ~ 2 there remains only a trace of the original 1600-cm^{-1} band, and the shoulder at 1623 cm^{-1} has developed into a clearly observable peak.

The initial shift of the carbonyl band at 1600 cm^{-1} to still lower wavenumbers and the absence of any band at 1623 cm^{-1} until the pH is 4 or lower both indicate that the addition of the first proton to ferric enterobactin causes a shift in the coordination of the iron from the two phenolic oxygens to the amide carbonyl and ortho phenolic oxygens, with concomitant protonation of the meta phenolate group. If the initial chelate protonation reaction were resulting in dissociation of a DHB side group, the carbonyl band at 1623 cm^{-1} would be expected to appear at about pH 5.

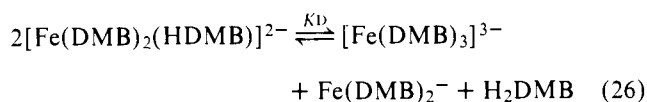
In the ferric MECAM system, where the first three chelate protonations occur cleanly, the carbonyl stretch completely disappears on addition of 3 equiv of acid, but there is no trace of an uncoordinated DHB band.¹⁷ Addition of 2 equiv of hydrogen ion to ferric enterobactin, on the other hand, yields a spectrum in which a weak shoulder at 1623 cm^{-1} indicates that a complex containing uncoordinated DHB is present, as well as the bis(salicylate) complex. Consistent with this observation, the spectrophotometric titrations indicate that below pH 4.2 there are several overlapping protonation equilibria.

Mode of Bonding in Enterobactin. The shift from catechol to salicylate binding (Scheme II) is understandable from simple resonance and entropic arguments. Llinas et al.²⁴ have concluded that conjugation of the ortho hydroxy with the amide carbonyl should result in a higher intrinsic acidity of the ortho hydroxyl group relative to the meta, and this is observed in such compounds as 2-hydroxybenzaldehyde ($\text{p}K = 8.1$) and 3-hydroxybenzaldehyde ($\text{p}K = 9.0$).²⁷ These results indicate that protonation should occur at the meta position first, with the remaining negative charge partially delocalized onto the carbonyl oxygen. The iron-oxygen bonding in such a system is expected to be stronger than that found for electronically isolated carbonyls, as is the case for acetylaceton complexes. Since there is negligible competition from hydrogen ion for the carbonyl binding site, metal binding to the carbonyl oxygen becomes more favorable relative to the very basic meta phenolate group as the pH is lowered. In the DMB system, the combination of the energy of the iron-carbonyl bond plus the positive ΔS associated with retaining a chelate ring are insufficient to compensate for the energy gain associated with protonation of the ortho phenolic group and dissociation of a DMB molecule. In the macrochelates, the iron-carbonyl bond energy is presumably the same as that in the DMB complex. However, the attachment of the DHB groups to a central ring means that dissociation of a DHB entails the loss of three chelate rings, and the increase in ΔS appears to be sufficient to prevent protonation of the ortho hydroxyl group until very low pH.

This explanation of salicylate bonding can be treated semiquantitatively on the basis of known equilibrium constants. One can estimate the "salicylate" binding constant of monoprotonated DMB from the reported values of salicylamide as:

The analogous constant for a "catecholate"-bound DMB (K_{cat}) is simply the K_{ML_3} (eq 6) described above, which is $10^{8.8}$. Given these values, a disproportionation constant can be calculated

for the reaction:



$$K_D = \frac{[\text{Fe}(\text{DMB})_3]^{3-}[\text{Fe}(\text{DMB})_2^-][\text{H}_2\text{DMB}]}{[\text{Fe}(\text{DMB})_2(\text{HDMB})]^{2-}]^2} = \frac{K_{\text{cat}} K_1^{\text{H}}}{(K_{\text{sal}})^2 K_2^{\text{H}}} \quad (27)$$

This value of K_D is quite low, so the main factor responsible for the absence of salicylate bonding in the DMB system is the concentration dependence of eq 26, which is driven to the right in dilute solutions.

With sexidentate ligands such as enterobactin, the increase in the ΔS for coordination of a dihydroxybenzoyl group that is covalently attached to the bis(catecholate) complex should increase both K_{sal} and K_{cat} . Since the $\log K_{\text{ML}}$ of enterobactin is almost 12 log units greater than the β_3 of DMB, K_{sal} and K_{cat} for the enterobactin complex should be ~ 5 – 6 log units higher than the DMB values. Because K_{sal} is squared in eq 17, this results in a disproportionation constant for the mono(salicylate)–ferric enterobactin complex of about 10^{-5} . This constant is defined as:

$$K_D = \frac{[\text{Fe}(\text{ent})^{3-}][\text{Fe}(\text{H}_2\text{ent})^-]}{[\text{Fe}(\text{Hent})]^2} \approx 10^{-5} \quad (28)$$

and has no concentration dependence. These results predict that only a few tenths of a percent of the $[\text{Fe}(\text{Hent})]^{2-}$ complex would disproportionate into bis- and tris(catecholate) complexes, resulting instead in the observed salicylate mode of coordination.

Recently a paper has appeared that reports titration data for the ferric complexes of catechol, *N*-methyl-2,3-dihydroxybenzamide, and enterobactin, the results of which are at significant variance with those reported here. It is clear that DMB forms discrete mono, bis, and tris complexes with ferric ion, as reflected in the Bjerrum plot in Figure 2 and by breaks in the potentiometric equilibrium curves at 2 and 4 equiv of base per mol of iron, and previous workers have reported qualitatively the same results for a variety of catecholate ligands.^{21,28,29} In contrast, the titration curve reported by Spiro et al.¹⁹ for the iron–catechol system shows a sharp break at about 2.75 equiv of base, then levels off at pH 11 after the addition of only 4 equiv of base. Their titration curve for the ferric complexes of *N*-methyl-2,3-dihydroxybenzamide is essentially a straight line from 1 to 6 equiv. These results are inconsistent with the formation of simple mono, bis, and tris complexes, and the catechol results would require the postulation of polynuclear species. We suspect that the 3:1 ligand-to-metal ratio used by Spiro et al. is not sufficient to keep all the ferric ion in solution under neutral or basic conditions.

There also exist discrepancies between the enterobactin data presented here and those reported by Spiro et al.,¹⁹ which show an exceedingly flat buffer region from 1 to 6 equiv of base, with the pH at $\alpha = 1$ still above 4. Such strong buffering between pH 4 and 5 would require that the complexation equilibrium be expressed as a single-step dissociation of $\text{Fe}(\text{ent})^{3-} + 6\text{H}^+ \rightleftharpoons \text{Fe}^{3+} + \text{H}_6\text{L}$, in contradiction to the spectrophotometric data presented here. Furthermore, no mention is made of the precipitation that invariably occurs in the ferric enterobactin system below pH 3.5. Finally, the extinction coefficient reported by Spiro et al.¹⁹ for the ferric tris(*N*-methyl-2,3-dihydroxybenzamide) complex (ϵ 1900) is unusually small for a tris(catecholate) complex, for which no value less than 4000 has been reported^{21,26,28,30} [e.g., $[\text{Fe}(\text{cat})_3]^{3-}$, ϵ 4190,²¹ $[\text{Fe}(\text{DMB})_3]^{3-}$, ϵ 4910 (this work)]. Similarly, the ferric enterobactin extinction coefficient reported by Spiro et al. is low

(ϵ 3200), both in comparison with other tris(catecholates) (vide supra) and with the previously reported values for ferric enterobactin.^{9,15} In short, the resonance Raman results of Spiro et al. provided no new information regarding the structure and bonding of enterobactin, and the titrimetric and spectrophotometric results are incorrect.

Formation Constants. Although the K^* value for ferric enterobactin reported above is a valid metal–ligand equilibrium constant, it is difficult to compare it to the normal formation constants tabulated for other complexes,^{21,27} which do not include protons. To express the equilibrium constant in the usual fashion, i.e., without proton dependence, requires knowledge of the experimentally inaccessible $\text{p}K_{\text{a}}$ s of enterobactin. Previously, we have observed that the three lower ligand protonation constants of triccatecholate enterobactin analogues tend to have an average value that is very close to that of the bidentate model DMB, with separations between successive constants of about 0.8 log unit.¹⁷ Thus, the logarithms of the three lower protonation constants of enterobactin can be reasonably estimated as 7.6, 8.4, and 9.2. A similar argument holds for the three higher ligand $\text{p}K_{\text{a}}$ s, and with these estimates, one can calculate a $\log K_{\text{ML}}$ for ferric enterobactin of 52, where K_{ML} is defined in the usual way as:

$$K_{\text{ML}} = \frac{[\text{Fe}(\text{ent})^{3-}]}{[\text{Fe}^{3+}][\text{ent}^{6-}]} \quad (29)$$

The value of 52, even though a rough estimate (± 1 log unit), is by far the highest formation constant ever measured for an iron complex and clearly indicates the tremendous stability of the enterobactin complex. This value is almost 27 orders of magnitude higher than the K_{ML} of EDTA, and is 6 log units greater even than the formation constant of ferric MECAM. In the latter compound the coordinating groups of both ligands are the same (six phenolic oxygens from three DHB groups); hence the intrinsic affinity of the individual ligating groups for ferric ion should be very similar. The large difference in $\log K_{\text{ML}}$ must therefore reflect a very stable ligand structure for enterobactin. The flexibility of the triester ring in enterobactin may be a factor in the large difference in stability between it and MECAM. Although MECAM actually has one additional atom between the central benzene ring and the exterior DHB groups, the rigid planarity of the central ring does not allow the α carbons to flex out of the plane toward the metal, which may introduce some strain into the ferric MECAM complex.

There is an increase of over 10 log units between the formation constants of ferric enterobactin and the tris(DMB) complex, a difference which cannot be accounted for by a classical chelate effect, i.e., one attributable to the favorable entropic contribution from displacing coordinated water molecules, which accounts only for an increase of 5–6 log units on going from a tris(bidentate) to a sexidentate complex.³¹ Rather, it appears that the exceptional stability of the ferric enterobactin complex is the result of two main factors. First, the cyclic triester base severely restricts the conformational freedom of the free ligand relative to a linear analogue. This should result in an unusually high ΔS for complex formation, since this freedom is normally lost only upon coordination to a metal ion and subtracts from the entropy gained in release of coordinated water. In addition, the large difference between the $\log K_{\text{ML}}$ values of enterobactin and MECAM appears to indicate that the flexibility of the central triester ring may be needed to avoid significant steric strain (an enthalpy change) in the formation of the ferric complex.

Comparison with Other Ligands. Although the K_{ML} values of catecholate complexes are quite large, the ligand protonation constants are also very large, so that as the pH is lowered, hydrogen ions compete effectively with ferric ion for the basic phenolic oxygens even at physiological pH; for example, iron

Table II. Free Metal Concentrations Expressed as $pM = -\log [Fe^{3+}]$ for pH 7.4 Solutions Containing 10^{-6} M Total Iron and 10^{-5} M Total Ligand

ligand	pM
enterobactin	35.6
MECAM ^a	29.1
ferrioxamine E	27.7
ferrioxamine B	26.6
N-acetylferrioxamine B	26.5
ferrichrysin	25.8
ferrichrome	25.2
diethylenetriaminepentaacetic acid	24.7
transferrin	23.6
aerobactin	23.3
rhodotorulic acid	21.9
2,3-dihydroxy-N,N-dimethylbenzamide	~15 ^b

^a See Figure 9. ^b Exceeds solubility product of ferric hydroxide, indicating precipitation under the prescribed conditions.

can be removed from enterobactin by EDTA at pH 5, despite the 27 order of magnitude difference in formation constants. Thus, it is important to have a measure of the iron binding ability that accounts for pH dependence. In the past, it has been common to use "effective" binding constants,³² which are usually defined as:

$$K_{\text{eff}} = \frac{[ML]}{\sum_{i=0}^2 [M(OH)_i] \sum_{j=0}^n [H_j L]} \quad (30)$$

However, definitions vary from worker to worker, leading to a considerable amount of confusion. In addition, it is difficult to define a K_{eff} that can account for all the variations between ligands. For example, transferrin has two irons per molecule of ligand and formation of the ferric complex depends on the carbonate concentration, while rhodotorulic acid forms an Fe_2L_3 dimer at physiological pH, and ferric aerobactin dissociates a citrate hydroxyl group between pH 4 and 6. As an alternative to effective binding constants, the relative abilities of various ligands to sequester ferric ion can be determined by calculating the equilibrium concentration of hexaaquoiron(III) in a solution of specified pH, total iron, total ligand, and carbonate concentrations. With this criterion, comparison between ligands is straightforward; a smaller free iron concentration, which means a larger pM ($pM = -\log [Fe^{3+}]$), indicates a more effective ligand. A list of the siderophore pM values is shown in Table II, along with the values for a few synthetic ligands. For the catecholate ligands the calculation of pM has the added advantage of being independent of the three most basic ligand protonation constants, rendering unnecessary the inherently inaccurate estimation of these values.

The values listed in Table II demonstrate that, at pH 7.4, enterobactin is by far the most effective siderophore characterized. The pM values for a number of synthetic ligands have also been determined, although only three are listed here, but none have been found which exceed the enterobactin pM, which is also several orders of magnitude greater than that of human serum transferrin. Obviously the enteric bacteria have evolved an extremely powerful iron sequestering agent, capable of competing both with other microorganisms and with mammalian hosts for ferric ion. It is also clear from the data in Table II that MECAM, though less powerful than enterobactin, is still a better ligand for Fe(III) at pH 7.4 than any of the hydroxamate siderophores, and is thermodynamically capable of quantitatively removing the iron from an equivalent concentration of transferrin. Perhaps equally important, MECAM and enterobactin are both kinetically facile in removing iron from transferrin under conditions in which des-

ferrioxamine, the current drug of choice for iron removal in man, is ineffective.³⁴

Conclusions

Our potentiometric and electrochemical results on ferric enterobactin establish the great avidity with which enterobactin binds Fe(III). Ferric enterobactin has a stability constant near 10^{52} , and enterobactin has been demonstrated to be the most effective iron chelator at physiological pH yet characterized, capable even of removing iron from transferrin. Bacteria employing enterobactin-mediated iron transport thus are able to compete effectively for iron both with other microorganisms and with the mammals within which they live. As a result of the specific and powerful sequestration of ferric ion, we observe an inordinately low reduction potential for ferric enterobactin, -1.230 V vs. SCE at pH 10. This is consistent with suggestions that ferric enterobactin has too low a reduction potential to be physiologically reducible, and consequently must be hydrolyzed to permit iron reduction and removal. At pH 7 the reduction potential of ferric enterobactin is calculated to be -750 mV vs. NHE.

Acknowledgments. We gratefully acknowledge the financial support of the National Institutes of Health through Grant No. AI 11744. We thank Dr. F. L. Weilt, of the Lawrence Berkeley Laboratory, for providing samples of the ligand DMB.

References and Notes

- (1) Previous paper in this series: Abu-Dari, K.; Freyberg, D. P.; Raymond, K. N. *Inorg. Chem.*, in press.
- (2) Biedermann, G.; Schindler, L. *Acta Chem. Scand.* **1957**, *11*, 731-740.
- (3) Neilands, J. B. "Inorganic Biochemistry"; Eichhorn, G., Ed.; Elsevier: Amsterdam, 1973; pp 167-202.
- (4) Neilands, J. B. *J. Am. Chem. Soc.* **1952**, *74*, 4846-4847.
- (5) Bullen, J. J.; Rogers, H. J.; Griffiths, E. "Microbial Iron Metabolism"; Neilands, J. B., Ed.; Academic Press: New York, 1974; pp 517-551.
- (6) O'Brien, I. G.; Gibson, F. *Biochim. Biophys. Acta* **1970**, *215*, 393-402.
- (7) Pollack, J. R.; Neilands, J. B. *Biochem. Biophys. Res. Commun.* **1971**, *38*, 989-992.
- (8) Langman, L.; Young, I. G.; Frost, G. E.; Rosenberg, H.; Gibson, F. *J. Bacteriol.* **1972**, *112*, 1142-1149.
- (9) O'Brien, I. G.; Cox, G. B.; Gibson, F. *Biochim. Biophys. Acta* **1971**, *237*, 537-549.
- (10) Bryce, G. F.; Weller, R.; Brot, N. *Biochem. Biophys. Res. Commun.* **1971**, *42*, 871-879.
- (11) Emery, T. *Biochemistry* **1971**, *10*, 1483-1488.
- (12) Kochan, I. "Bioinorganic Chemistry—II"; Raymond, K. N., Ed.; American Chemical Society: Washington, D.C., 1977; pp 55-77.
- (13) Cooper, S. R.; McArdle, J. V.; Raymond, K. N. *Proc. Natl. Acad. Sci. U.S.A.* **1978**, *75*, 3551-3554.
- (14) Harris, W. R.; Carrano, C. J.; Raymond, K. N. *J. Am. Chem. Soc.*, **1979**, *101*, 2213-2214.
- (15) Anderson, B. F.; Buckingham, D. A.; Robertson, G. B.; Webb, J.; Murray, K. S.; Clark, D. E. *Nature (London)* **1976**, *262*, 722.
- (16) Greenwood, J. T.; Luke, R. K. *J. Biochim. Biophys. Acta* **1978**, *525*, 209-218.
- (17) Harris, W. R.; Raymond, K. N., *J. Am. Chem. Soc.* in press.
- (18) Johnson, R. R. "Elementary Statistics"; Duxbury Press: North Scituate, Mass., 1973; p 267.
- (19) Salama, S.; Strong, J. D.; Neilands, J. B.; Spiro, T. G. *Biochemistry* **1978**, *17*, 3781-3785.
- (20) Nicholson, R. S.; Shain, I. *Anal. Chem.* **1964**, *36*, 706-723.
- (21) Avdeef, A.; Sofen, S. R.; Bregante, T. L.; Raymond, K. N. *J. Am. Chem. Soc.* **1978**, *100*, 5362-5370.
- (22) Harris, W. R.; Weilt, F. L.; Raymond, K. N. *J. Chem. Soc., Chem. Commun.*, **1979**, 177-178.
- (23) Tait, G. H. *Biochem. J.* **1975**, *146*, 191-204.
- (24) Llinas, M.; Wilson, D. M.; Neilands, J. B. *Biochemistry* **1973**, *12*, 3836-3843.
- (25) Motekaitis, R. J.; Martell, A. E. *J. Am. Chem. Soc.* **1970**, *92*, 4223-4230.
- (26) Motekaitis, R. J.; Martell, A. E. *Inorg. Chem.* **1974**, *13*, 550-559.
- (27) Martell, A. E.; Smith, R. M. "Critical Stability Constants"; Plenum Press: New York, 1977; Vol. III.
- (28) Murakami, Y.; Nakamura, K. *Bull. Chem. Soc. Jpn.* **1963**, *36*, 1408-1411.
- (29) Willi, A.; Schwarzenbach, G. *Helv. Chim. Acta* **1951**, *34*, 528-539.
- (30) Corey, E. J.; Hurt, S. D. *Tetrahedron Lett.* **1977**, *45*, 3293-3294.
- (31) Martell, A. E. *Adv. Chem. Ser.* **1967**, No. 62, 272-294.
- (32) Pitt, C. G.; Gupta, G. Washington, D.C., 1975, DHEW Publication No. (NIH) 77-994, pp 137-168.
- (33) Aisen, P.; Leibman, A.; Zweier, J. *J. Biol. Chem.* **1978**, *253*, 1930-1937.
- (34) Carrano, C. J.; Raymond, K. N. *J. Am. Chem. Soc.* in press.